2018년 2월
박사학위 논문

광범위B대세포림프종의 세포기원 규명을 위한 Lymph2Cx 분석과 Hans 알고리즘의 비교

조선대학교 대학원
의 학 과
조 인 주

광범위B대세포림프종의 세포기원 규명을 위한 Lymph2Cx 분석과 Hans 알고리즘의 비교

Comparison of Lymph2Cx Assay and Hans Algorithm to Determine the Cell-of-Origin of Diffuse Large B-cell Lymphomas

2018년 2월 23일

조선대학교 대학원
의 학 과
조 인 주

광범위B대세포림프종의 세포기원 규명을 위한 Lymph2Cx 분석과 Hans 알고리즘의 비교

지도교수 이 미 자

이 논문을 의학 박사학위신청 논문으로 제출함

2017년 10월

조선대학교 대학원
의 학 과
조 인 주

조인주의 박사학위논문을 인준함

위원장 조선대학교 교수 기근홍 (인)

위 원 성균관대학교 교수 고영혜 (인)

위 원 조선대학교 교수 임성철 (인)

위 원 조선대학교 교수 홍 란 (인)

위 원 조선대학교 교수 이미자 (인)

2017년 12월

조선대학교 대학원

목 차

표 목 차

도 목 차

초록

광범위B대세포림프종의 세포기원 규명을 위한 Lymph2Cx 분석과 Hans 알고리즘의 비교

조인주
지도교수: 이미자
조선대학교 대학원 의학과

광범위B대세포림프종에서 표적치료의 선택 및 예후인자 확인을 위한 세포기원을 결정해 주는 것이 중요해지고 있다. Hans 알고리즘에 따른 면역조직화학적 염색을 통한 방법이 널리 이용되지만, 최근에는 리보핵산을 통한 유전자 발현을 이용하여 세포기원을 결정하는 Lymph2Cx 분석이 개발되어 활발히 연구 중이다. 하지만 두 방법 사이의 불일치 율이 보고되고 있어 본 연구에서 이들 사이의 불일치되는 그룹과 Lymph2Cx의 미분류 그룹에 대하여 분석하고자 하였다.

전체 179례의 광범위B대세포림프종에서 Hans 알고리즘을 통해 58 증례(32.4%)가 배아중심 B세포류 타입으로, 121 증례(67.6%)가 비배아중심 B세포류 타입으로 분류되었다. 전체적인 일치도는 74.9%이었으며, 불일치되는 증례들은 Hans 알고리즘에 의한 배아중심 B세포류 타입에서 더 높게 분포(20.7%) 하였다. 전체 22례의 불일치 증례들 중에서, 12 증례(54.5%)의 배아중심 B세포류 타입은 Lymph2Cx 분석에서 비배아중심 B세포류 타입이었으며, 면역조직화학적 염색별로 살펴보았을 때, CD10-/BCL6+ Hans 알고리즘에 의한 배아중심 B세포류 타입이 다른 면역조직화학적 염색 타입들보다 더 높았다. 또한 Lymph2Cx 는 23례의 증례(12.85%)를 미분류 그룹으로 지정하였으며, 림프절외 림프종이 림프절 림프종 보다 의미 있게 더 높은 비율을 차지하고 있었다.

본 연구결과 Lymph2Cx 는 광범위B대세포림프종에서 세포기원을 결정하는데 있어, Hans 알고리즘의 제한점을 극복할 수 있는 더 나은 방법임을 확인하였으며, Hans 알고리즘을 통하여 세포기원을 결정하는데 있어 유의해야할 면역조직화학적 염색 타입을 분석하였다는 점에서 의미가 있을 것으로 판단된다.

핵심어: 광범위B대세포림프종, 세포기원, Lymph2Cx 분석, Hans 알고리즘

Ⅰ. Introduction

Diffuse large B-cell lymphoma (DLBCL) is the most common subtype of non-Hodgkin lymphoma, characterized by heterogeneity, not only with respect to clinical presentation and morphology, but also for molecular pathogenesis and gene expression (1, 2). Most patients with DLBCL have no known underlying risk factors. A minority of cases occur in the setting of congenital immunodeficiency or acquired immunodeficiency (3). Most patients present with rapidly growing lymph nodes or tumor masses in extranodal sites. The median age of the patients is 64 years, but any age can be affected. There is a slight male predominance (3).

Studies on the molecular pathogenesis of DLBCL using DNA microarray have documented diverse gene expression in the tumors of DLBCL patients, which seem to arise from B cell at different stages of differentiation (1). According to gene expression profiles, these molecularly distinct subtypes were termed as germinal-center B-cell-like (GCB) DLBCL and activated B-cell-like (ABC) DLBCL (1, 4). These subtypes were different, not only in their gene expression profiles, but also in overall survival following standard treatments (1, 5, 6). GCB DLBCL patients respond well to combined chemotherapy with the anti-CD20 antibody Rituximab, whereas more than 50% of the ABC DLBCL patients succumb to their disease (1, 6). Constitutive activation of the nuclear factor-kappa B (NF-κB) signaling pathway, in order to block apoptosis, plays an important role in the molecular pathogenesis of ABC DLBCL (1, 7). This led to the introduction of novel therapeutic strategies that selectively targeted the biological activities of each molecular subtype. Several clinical trials demonstrated the role of agents

such as Ibrutinib (8) and Lenalidomide (9, 10) in targeting the ABC DLBCL oncogenic pathway.

It is well-documented that GCB type DLBCL shows significantly better overall survival than ABC type DLBCL as per gene expression profile (GEP) classification (4, 11-14). Besides prognostic significance, determination of the COO for DLBCL is also important for selecting target therapy. Although GEP using DNA microarray platform is considered as gold standard of determining COO for DLBCL, the issues of tissue requirement (fresh or frozen tissue), complexity, and low reproducibility have led to develop various molecular methods adaptable to fresh frozen paraffin-embedded (FFPE) tissue (3).

Various immunohistochemistry (IHC) based approaches for the molecular classification in DLBCL have been introduced. In 2005 Hans and co-workers (10) established the first IHC algorithm, with supposed high sensitivity for GEP classification. Hans *et al.* determined the COO for DLBCLs into GCB type versus non-GCB (or ABC) type using IHC expression of CD10, BCL6, and MUM1 with ≥30% of expression considered as positive (15). According to Hans algorithm, CD10+ or CD10- with BCL6+/MUM1- are classified as GBC type of DLBCL. Also, CD10- with BCL6+/MUM1+ or CD10- with BCL6- are classified as non-GCB (or ABC) type of DLBCL (15). Subsequently, eight further algorithms have been published including Choi algorithm (16), and all of them reported better concordance with molecular-based classification and ability to segregate two groups with different outcome (3). However, the correlation with GEP results is imperfect, with concordance rate of 75% to 90% (3). Moreover, the unclassified group by GEP cannot be recognized by immunophenotyping, therefore such cases will likely be forced into either GCB or non-GCB type (3).

To overcome the issues of GEP by DNA microarray platform and immunophenotyping algorithms, various molecular methods adaptable to FFPE tissue have been developed. The most promising method among them is Lymph2Cx assay of twenty genes using NasoString platform. Lymph2Cx assay analyzes a limited panel of genes based on data from gene-expression studied to distinguish the GCB and ABC groups and establish signatures of prognostic significance (3).

It is well documented that the COO determined by the Lymph2Cx assay maintained the same prognostic significance (17, 18). In a previous study conducted by Yoon *et al*. (14), Lymph2Cx-assigned ABC type patients had significantly worse outcome than GCB type patients, in which the COO determined by the Hans algorithm did not show significant difference (14).

Overall correlation of Lymph2Cx and Hans algorithm is described in other studies (14, 17, 19), but the detailed characteristics of discordant cases and unclassified group of Lymph2Cx remain elusive. Therefore, we compared the COO assigned by Lymph2Cx and the Hans algorithm in DLBCL patients. Concordant and discordant groups between the two were analyzed, and the unclassified group determined by Lymph2Cx was documented. Furthermore, the characteristics and IHC staining patterns of each groups classified by the Hans algorithm and those of cases showing discrepancy were reviewed. By documenting the possible causes of discrepancy, this study aimed to improve the guidelines in determining COO of DLBCL via the Hans algorithm.

II. Materials and Methods

A. Patients

We retrospectively evaluated 187 patients with DLBCL in the Samsung Medical Center between 2015 and 2017. Two pathologists (I. Cho and Y. Ko) reviewed the histopathology slides of the patients according to the 2008 WHO classification. Of 187 patients, representative FFPE tissues of 179 cases were selected from the archived histopathology files of the Samsung Medical Center and medical records were reviewed for clinical information.

B. Cell-of-origin determined by the Lymph2Cx assay

NanoString-based multigene assay was performed according to the methods described by Scott *et al*. (17) and Yoon *et al*. (14). High Pure RNA Paraffin kits (Roche Diagnostic, Mannheim, Germany) were used to extract total RNA from 4-μm thick sections of FFPE tumor tissues. Nucleic acids were extracted using Qiagen AllPrep FFPE kits (Qiagen, Hilden, Germany), and digital GEP was performed on 200 ng aliquots of RNA using NanoString technology. Gene expression analyses were carried out using the Lymph2Cx code set (NanoString Technologies, Seattle, WA, USA). After normalization of the data, standard QC was performed using the nSolver™ Analysis Software (NanoString Technologies, WA). Normalization was done using the mean expression level value of the internal reference genes with a cut-off value of 20. Data processing and COO-type assignment were done through the website https://llmpp.nih.gov/LYMPHCX/index.shtml.

C. Cell-of-origin determined by the Hans algorithm using immunohistochemical staining of CD10, BCL6 and MUM1

Immunohistochemical (IHC) staining of CD10 (Novocastra, NCL-L-CD10-270, Mouse monoclonal, 1:100 dilution), BCL6 (Novocastra, NCL-L-Bcl-6-564, Mouse monoclonal, 1:40 dilution), and MUM1 (Dako, M7259, Mouse monoclonal, 1:200 dilution) was performed at the time of diagnosis. FFPE tissue sections (4-μm thick) were stained automatically (Technomate 1000, DakoCytomation, DAKO, Glostrup, Denmark) using standard methods. The slides were semi-quantitatively analyzed by two pathologists (I. Cho and Y. Ko). Based on the Hans algorithm, CD10, BCL6, and MUM1 expression levels were evaluated. The expression level of ≥30% were considered as positive. MUM1 expression level of 30% were classified as borderline MUM1 expression and MUM1 expression level >30% were classified as definite MUM1 expression. For discordant cases, an agreement was reached by a joint review on a multi-head microscope.

D. Statistical analysis

Statistical evaluation was carried out by using the SPSS ver. 21 software (SPSS, Inc., Chicago, IL, USA). Fisher's exact test and chi-square test was used to demonstrate the clinicopathologic correlation between the COO types as determined by the Lymph2Cx assay and Hans algorithm. Wilcoxon-Mann-Whitney test was used to demonstrate the distribution of ABC likelihood score in the Lymph2Cx unclassified group. A proportion z-test was performed to evaluate the proportion of the unclassified group as categorized by

Lymph2Cx and the discordant group between Lymph2Cx and the Hans algorithm. The P value less than 0.05 was considered to be statistically significant.

III. Results

Our studied cohort included 106 (59.2%) male and 73 (40.8%) female patients (M : F ratio, 1.5:1), with a mean age of 59 years (range, 28-92). About two-thirds (65.9%) of the cohort had extranodal lymphomas and the rest had nodal lymphomas (34.1%). One-third

Table 1. Clinicopathologic features and the association between the cell-of-origin determined by the Hans algorithm and Lymph2Cx assay

Clinicopathologic features	Total (n=179)	Hans algorithm, n (%)			Lymph2Cx, n (%)			
		GCB (n=58, 32.4%)	Non-GCB (n=121, 67.6%)	P-value	GCB (n=46, 25.7%)	ABC (n=110, 87.2%)	Unclassified (n=23, 12.8%)	P-value
Sex								
Male	106 (59.2)	41 (70.7)	65 (53.7)	0.031	31 (67.4)	60 (54.5)	15 (65.2)	0.271
Female	73 (40.8)	17 (29.3)	56 (46.3)		15 (32.6)	50 (45.5)	8 (34.8)	
Primary site								
Nodal	61 (43.1)	19 (32.8)	42 (34.7)	0.796	17 (37.0)	41 (37.3)	3 (13.0)	0.074
Extranodal	118 (65.9)	39 (67.2)	79 (65.3)		29 (63.0)	69 (62.7)	20 (87.0)	
Age, years								
≤ 60	85 (47.5)	28 (48.3)	57 (47.1)	0.884	22 (47.8)	52 (47.3)	11 (47.8)	0.997
> 60	94 (52.5)	30 (51.7)	64 (52.9)		24 (52.2)	58 (52.7)	12 (52.2)	
Specimen type								
Excision	58 (32.4)	23 (39.7)	35 (28.9)	0.151	20 (43.5)	30 (27.3)	8 (34.8)	0.138
Biopsy	121 (67.6)	35 (60.3)	86 (71.1)		26 (56.6)	80 (72.7)	15 (65.2)	
Needle	41 (33.9)	9 (22.0)	32 (78.0)		8 (19.5)	31 (75.6)	2 (4.9)	
Endoscopic	23 (19.0)	11 (47.8)	12 (52.2)		10 (43.5)	11 (47.8)	2 (8.7)	
Non-needle, non-endoscopic	57 (47.1)	15 (26.3)	42 (73.7)		8 (14.0)	38 (66.7)	11 (19.3)	

Note: COO, cell of origin; ABC, activated B cell; GCB, germinal center B cell.

(32.4%) of the cases were excised specimens and the rest (67.6%) were biopsied ones. Of the biopsied specimens, 33.9% were needle-biopsied, 19% were endoscopically-biopsied, and the rest (47.1%) were non-needle/non-endoscopically-biopsied (including incisional, excisional, punch biopsy, etc.) Clinicopathologic features and the COO association between Lymph2Cx and the Hans algorithm are summarized in Table 1.

A. Cell-of-origin classified by the Lymph2Cx assay and its comparison with the Hans algorithm

COO classification by the Lymph2Cx assay and Hans algorithm is summarized in Table 2. Of the 179 submitted patients, Hans algorithm classified 58 cases (32.4%) as GCB type and 121 cases (67.6%) as non-GCB type. Lymph2Cx assay assigned 46 cases (25.7%) as GCB type, 110 cases (61.5%) as ABC type, and 23 cases (12.8%) as intermediate/unclassified type. Of the 58 GCB type cases determined by the Hans algorithm, 36 cases (62.1%) were classified as GCB type, 12 cases (20.7%) as ABC type, and 10 cases (17.2%) as intermediate/unclassified by the Lymph2Cx assay. Of the 121 non-GCB type cases determined by the Hans algorithm, 98 cases (81.0%) were classified as ABC type, 10 cases (8.3%) as GCB type, and 13 cases (10.7%) as intermediate/unclassified by the Lymph2Cx assay. A statistically significant correlation ($p < 0.001$) was observed between the Hans algorithm and Lymph2Cx assay. The overall agreement between the COO determined by the Hans algorithm and Lymph2Cx assay was 74.9% and overall discrepancy rate was 25.1% (the rate was 14.1% if the Lymph2Cx unclassified type was excluded). The overall concordance rate was higher in non-GCB (ABC) type determined by the Hans algorithm (81% vs 62.1%).

Table 2. Cell-of-origin determined by the Lymph2Cx assay and its comparison with the Hans algorithm

		Lymph2Cx, n (%)			
		GCB (n = 46)	ABC (n = 110)	Unclassified (n = 23)	P-value
Hans algorithm, n (%)	GCB (n = 58)	36 (62.1)	12 (20.7)	10 (17.2)	< 0.001
	Non-GCB (n = 121)	10 (8.3)	98 (81.0)	13 (10.7)	

Note: COO, cell of origin; ABC, activated B cell; GCB, germinal center B cell.

B. Discordance between the Lymph2Cx assay and Hans algorithm

Twenty-two discordant cases were observed out of 179 cases. Twelve (54.5%) GCB type cases and 10 (45.5%) non-GCB type cases determined by the Hans algorithm were classified as ABC type and GCB type, respectively, by the Lymph2Cx assay. The characteristics and their association with the discordant cases are summarized in Table 3. Four excised specimen cases were lymph node excisions. Of the 18 biopsied specimen cases, 6 cases were endoscopically-biopsied and 4 cases were needle-biopsied. None of these clinicopathologic characteristics comprised significantly higher proportion in discordant group except for the COO determined by the Hans algorithm ($p = 0.027$). Especially, GCB type determined by the Hans algorithm exhibited significant proportion than non-GCB type (z-score = 2.22; $p = 0.027$). Of the 12 GCB type cases determined by the Hans algorithm, 5 cases (41.7%) revealed CD10 positivity, and 7 cases (58.3%) showed CD10-/BCL6+/MUM1-(BCL6 only positive). Of the 10 non-GCB type cases determined by the Hans algorithm, 4 cases (40%) revealed borderline MUM1 expression (MUM1 expression level of

30%), and 6 cases (60%) revealed definite MUM1 expression (MUM1expression level range of 40-90%). Nine out of ten cases revealed CD10 negativity with a BCL6 expression range of 30-90% (Figure 1).

Table 3. Clinicopathologic features and their correlation with the discordant group

Clinicopathologic features	Total, n = 179 (%)	Discordant group, n = 22 (%)	z-score (P-value)
Sex			0.86 (0.392)
Male	106 (59.2)	15 (68.2)	
Female	73 (40.8)	7 (31.8)	
Primary site			0.68 (0.499)
Nodal	61 (43.1)	9 (40.9)	
Extranodal	118 (65.9)	13 (59.1)	
Age, years			0.66 (0.507)
≤ 60	85 (47.5)	12 (54.5)	
> 60	94 (52.5)	10 (45.5)	
Specimen type			1.43 (0.154)
Excision	58 (32.4)	4 (18)	
Bx	121 (67.6)	18 (82)	
Type: Needle Bx	41 (33.9)	4 (18.2)	
Endoscopic Bx	23 (19)	6 (27.3)	
Non-needle, non-endoscopic Bx	57 (47.1)	8 (36.4)	
Site: Lymph node	28 (23.1)	5 (22.7)	
Stomach	12 (9.9)	4 (18.2)	
Brain	20 (16.5)	3 (13.6)	
Tonsil	15 (12.4)	2 (9.1)	
Head & Neck	17 (14.0)	2 (9.1)	
Others	29 (24.0)	2 (9.1)	
COO determined by Hans algorithm			2.22 (0.027*)
GCB	58 (32.4)	12 (54.5)	
Non-GCB	121 (67.6)	10 (45.5)	

Note: COO, cell of origin; ABC, activated B cell; GCB, germinal center B cell; Bx, biopsy; *, P < 0.05

Figure 1. Immunohistochemical profile of discordant group and its representative cases.

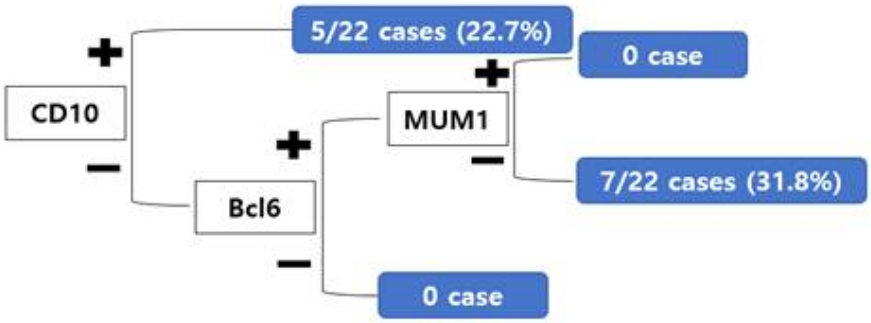

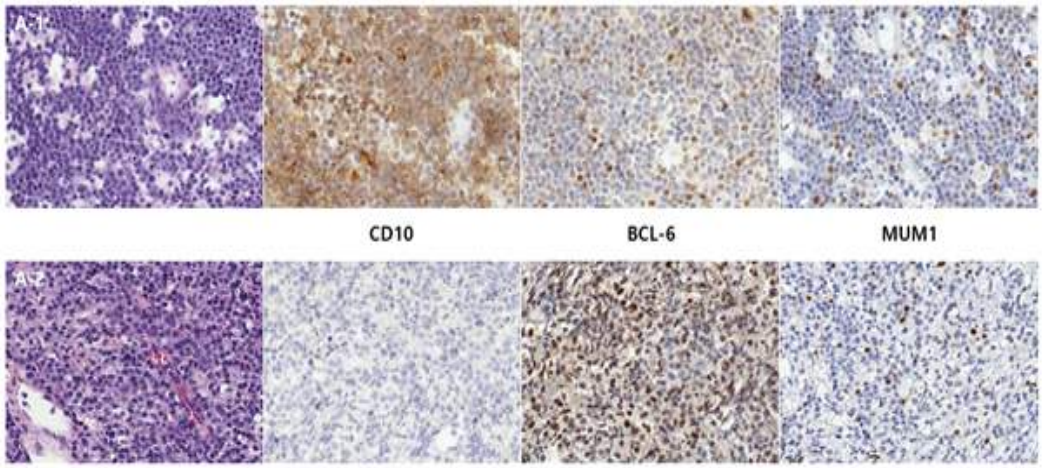

A. Immunohistochemical profile of GCB type determined by Hans algorithm in the discordant group (n=12/22, 54.5%). Of 12 cases of GCB-type determined by Hans algorithm, 5 cases (41.7%) revealed CD10 positivity, and 7 cases (58.3%) showed CD10 negativity and BCL6 positivity (BCL6 only positive). **A-1)** GCB type determined by Hans algorithm showing CD10+ (x400) **A-2)** GCB type determined by Hans algorithm showing CD10-/BCL6+/MUM1- (x400).

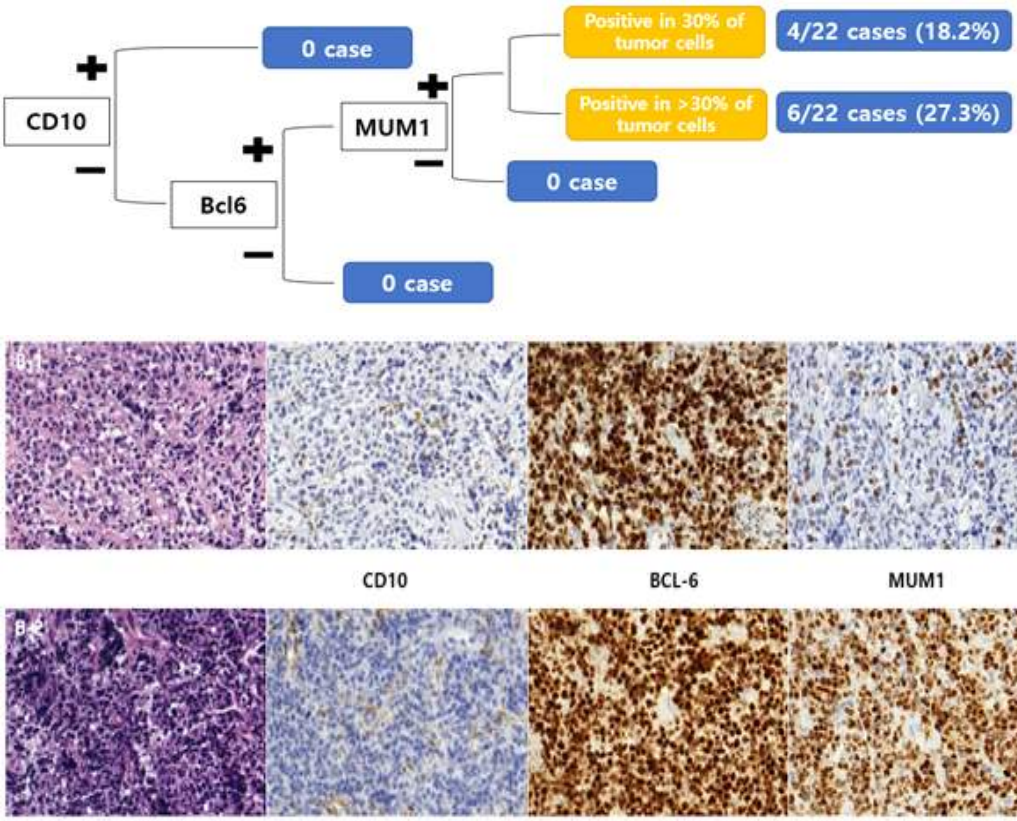

B. Immunohistochemical profile of the non-GCB type determined by Hans algorithm in the discordant group (n=10/22, 45.5%). Of 10 cases of non-GCB type determined by Hans algorithm, 4 cases (40%) revealed borderline MUM1 expression and 6 cases (60%) revealed definite MUM1 expression. **B-1)** Non-GCB type determined by Hans algorithm showing CD10-/BCL6+/borderline MUM1 expression (x400). **B-2)** Non-GCB type determined by Hans algorithm showing CD10-/BCL6+/definite MUM1 expression (x400).

C. Intermediate/unclassified subgroup in the Lymph2Cx assay

Of 179 cases, Lymph2Cx assay categorized 23 cases (12.9%) as intermediate/unclassified type. The clinicopathologic characteristics and their correlation with the Lymph2Cx unclassified group are summarized in Table 4. The proportion of extranodal lymphoma was significantly higher than nodal lymphoma (z-score = 2.13; p = 0.033). The 20 extranodal site specimens included the brain (n = 4, 17.4%), tonsils (n = 4, 17.4%), soft tissue (n = 3, 13%), stomach (n = 2, 8.7%), head & neck (n = 2, 8.7%), and one case each (n = 1, 4.3%) of the testis, cecum, colon, adrenal gland, and bone marrow. With regard to the IHC profile of the unclassified group, 10 cases (43.5%) were determined to be GCB type and 13 (56.5%) were non-GCB type by the Hans algorithm. Of the 10 GCB type cases determined by the Hans algorithm, only 3 cases were CD10 positive, while the rest were CD10-/BCL6+/MUM1-. Of the 13 non-GCB type cases determined by the Hans algorithm, one case exhibited borderline MUM1 expression, and the rest exhibited a definite MUM1 expression (MUM1 expression level range of 50-95%) (Figure 2). Moreover, no lean distribution was observed for ABC likelihood score in the Lymph2Cx unclassified group (Figure 3).

Table 4. Clinicopathologic features and their correlation with the Lymph2Cx unclassified group

Clinicopathologic features	Total, n = 179 (%)	Unclassified group, n = 23 (%)	z-score (P-value)
Sex			0.59 (0.558)
Male	106 (59.2)	15 (65.2)	
Female	73 (40.8)	8 (34.8)	
Primary site			2.13 (0.033*)
Nodal	61 (43.1)	3 (13.0)	
Extranodal	118 (65.9)	20 (87.0)	
Age, years			0.03 (0.974)
≤ 60	85 (47.5)	11 (47.8)	
> 60	94 (52.5)	12 (52.2)	
Specimen type			0.24 (0.807)
Excision	58 (32.4)	8 (34.8)	
Bx	121 (67.6)	15 (65.2)	
Type: Needle Bx	41 (33.9)	2 (8.7)	
Endoscopic Bx	23 (19)	2 (8.7)	
Non-needle, non-endoscopic Bx	57 (47.1)	11 (47.8)	
Site: Brain	20 (16.5)	4 (17.4)	
Tonsil	15 (12.4)	3 (13)	
Soft tissue	7 (5.8)	3 (13)	
Stomach	12 (9.9)	2 (8.7)	
Head & Neck	17 (14.0)	2 (8.7)	
Others	50 (41.3)	1 (4.3)	
COO by Hans algorithm			1.14 (0.256)
GCB	58 (32.4)	10 (43.5)	
Non-GCB	121 (67.6)	13 (56.5)	

Note: COO, cell of origin; ABC, activated B cell; GCB, germinal center B cell; Bx, biopsy; *, P < 0.05.

Figure 2. Immunohistochemical profile of Lymph2Cx unclassified group and its representative cases. Of 10 cases of GCB type determined by Hans algorithm, seven cases were BCL6 positive with CD10 and MUM1 negative, and the rest were CD10 positive. Of 13 cases of non-GCB type determined by Hans algorithm, one case showed borderline MUM1 expression, the rest revealed definite MUM1 expression.

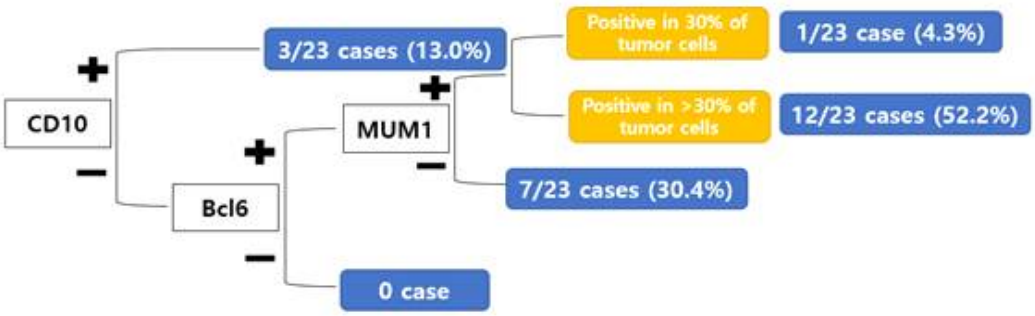

(Figure 2 continued in the next page)

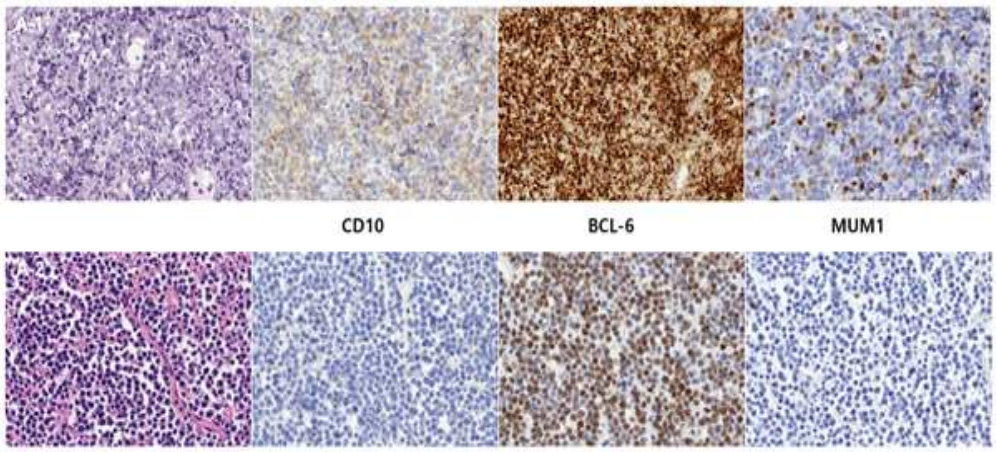

A-1) GCB type determined by Hans algorithm showing weak but diffuse CD10+ (x400). **A-2)** GCB type determined by Hans algorithm showing CD10-/BCL6+/MUM1- (x400).

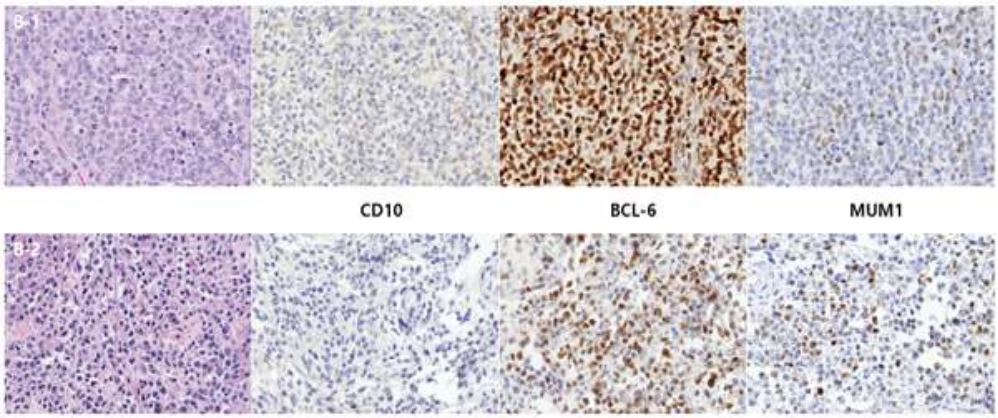

B-1) Non-GCB type determined by Hans algorithm showing CD10-/BCL6+/borderline MUM1 expression (x400). **B-2)** Non-GCB type determined by Hans algorithm showing CD10-/BCL6+/definite MUM1 expression (x400).

Figure 3. Distribution of ABC likelihood score of the Lymph2Cx unclassified group.

Wilcoxon-Mann-Whitney test revealed an ABC likelihood score range of 0.11-0.90 (median, 0.46, P > 0.05) without difference in median value between GCB and non-GCB type by Hans algorithm.

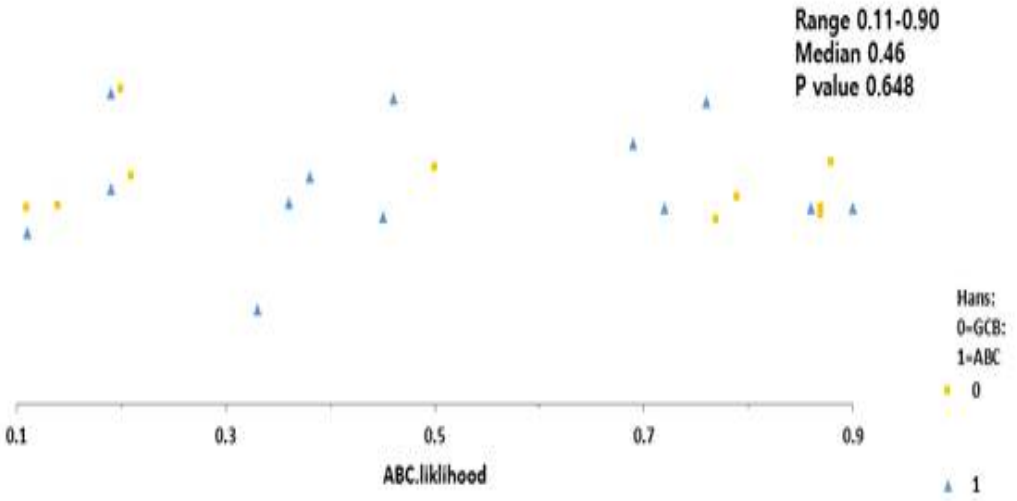

D. Discrepancy rate based on clinicopathologic features

The discrepancy rate in notable clinicopathologic characteristics was evaluated based on the clinicopathologic features of the discordant cases and the Lymph2Cx unclassified cases. Moreover, the discrepancy rate of different IHC profile in the Hans algorithm was analyzed. The overall discrepancy rate (including the discordant cases and Lymph2Cx unclassified cases) was observed to be 25.1%. The discrepancy rate of biopsied specimens was higher than excision specimens (27.3% vs 20.7%). Among the biopsied specimens, endoscopically-biopsied specimen revealed a higher discrepancy rate (26.1%) when compared to needle-biopsied specimen (14.6%) or the other non-needle/non-endoscopically-biopsied specimen (14.0%). Extranodal site specimens also showed a higher discrepancy rate (30.0%) than nodal site specimens (19.7%). With regard to the discrepancy rate of the IHC profiles, CD10-/BCL6+/MUM1- (BCL6 only positive) GCB type by Hans algorithm revealed the highest discrepancy rate (66.7%) when compared to other IHC profiles. The discrepancy rate of the CD10+/MUM1+ GCB type by Hans algorithm was 38.5%, borderline MUM1 expression non-GCB type by Hans algorithm was 23.5%, and definite MUM1 expression non-GCB type by Hans algorithm was 17.3%. Among these features, BCL6 only positive GCB type by Hans algorithm revealed statistically significant discrepancy rate (z-score = 4.07, $p < 0.001$; Figure 4).

Figure 4. Discrepancy rate based on clinicopathologic & immunohistochemical profile features. The proportional z-test revealed the BCL6+ only Hans GCB cases to be the only statistically significant feature among the other clinicopathologic and immunohistochemical profile features.

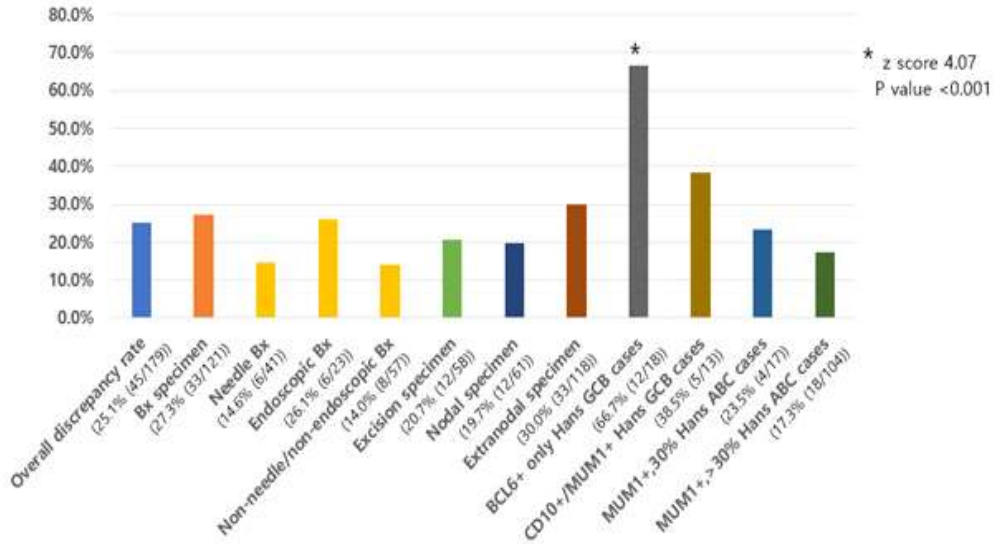

IV. Discussion

As approved targeted therapies that provide survival benefits to DLBCL patients emerge, accurate classification of the COO in DLBCL patients becomes more important. Molecular classification of DLBCL into the GCB and ABC subtypes is recommended in pathology established by the most recent WHO classification of the lymphoid neoplasm system (20). Although microarray GEP approach is considered to be the standard method for classifying COO in DLBCL (4, 11, 21), the issues of cost, availability, analytic preference for fresh frozen tissues, and lack of standardization in COO phenotype classification (14, 21) hinders its application in clinical practices where FFPE samples are widely used.

To overcome the above mentioned issues, the NanoString Technologies nCounter platform was developed (22-24). This digital GEPplatform enables multiplexed analysis of biomarkers from limited amounts of poor-quality material (22). The automated nCounter platform hybridizes fluorescent barcodes directly to specific nucleic acid sequences, facilitating the nonamplified measurement of up to 800 targets within one sample (23, 25). Previous studies reported that this platform offered high sensitivity, reproducibility, and full quantitative results for FFPE and frozen tissue samples (14, 18, 22, 23). Scott *et al*. (17) designed the NanoString-based test for COO assignment in FFPE tissues, and several studies validated its potential as a robust, highly-accurate, and feasible method in molecular COO distinction during routine diagnostic workflow (14, 17-19, 26).

Although GEP is the standard method for evaluating COO in DLBCL, cost-effective and readily-available IHC phenotype classification

is more widely adopted in clinical practice and prospective trial designs (14-16, 21, 27). The Hans algorithm classifies cases into GCB or non-GCB based on the sequential protein expression CD10, BCL6, and MUM1. This algorithm shows about 80% concordance correlation and similar survival outcomes with the GEP-defined subtype (15). Subsequent IHC algorithms with minor modifications have been developed to enhance performance (16, 27). The Choi algorithm incorporates FOXP1 and GCET1, and shows a 93% concordance rate with the GEP classification (16), whereas the Tally method substitutes BCL6 for LMO2 (27).

Despite its availability, the misclassification rate of the Hans algorithm has been reported to be 19.7% when compared to the GEP (28, 29). This probably arises from technical factors related to staining, interpretation, and data scoring (28, 29), especially in the variability of staining and scoring BCL6 (28, 30). However, Barrans *et al*. (31) pointed out that the decision tree of typing via an immunohistochemical algorithm, which uses sequential rather than parallel consideration of the immunopanel, inherently fails to capture the overall pattern of gene expression, which is reflected in clinical correlations (31). Several studies demonstrated similar patterns of discrepancy in COO determined via GEP and IHC-defined subtypes (12, 31). In a previous study conducted by Yoon *et al*. (14), the discrepancy rate between the Hans algorithm and Lymph2Cx assay was observed to be 26.4%, whereas our study showed 25.1% discrepancy (14.1% when excluding the Lymph2Cx unclassified group). The overall concordance rate was observed to be 74.9%, but the concordance rate of the GCB type determined by the Hans algorithm was lower than the non-GCB type (62.1% vs 81%). Moreover, GCB type determined by CD10-/BCL6+ showed the least concordance rate ($p = 0.04$). Other notable IHC profiles interpreted by the Hans algorithm

are the CD10+/MUM1+ cases and BCL6+ only (CD10-/BCL6+/MUM1-) cases, which are assigned as GCB type by definition. Thirteen cases of CD10+/MUM1+ GCB type were determined by the Hans algorithm, of which 2 cases were classified as ABC type and 3 cases were assigned as unclassified by the Lymph2Cx assay. The discrepancy rate was observed to be 38.5% (20.0% when excluding the unclassified group), which was slightly higher than the overall discrepancy rate without statistical significance. Eighteen cases of BCL6+ only (CD10-/BCL6+/MUM1-) GCB type cases were determined by the Hans algorithm, of which 7 cases were classified as ABC type and 5 cases were assigned as unclassified by the Lymph2Cx assay. The discrepancy rate was observed to be 66.7% (53.9% when excluding the unclassified group), both of which were statistically higher than the overall discrepancy (z-score = 4.07, $p < 0.001$). These results are supported by the previous study conducted by de Jong *et al.* (28), which reported poor interobserver/interlaboratory agreement for both BCL6 and MUM1 staining, even though CD10 staining and scoring was quite robust (28, 32). In the present study, we also re-reviewed the slides of the 22 discordant cases and verified the histologic characteristics of the discordant cases. Eighteen out of the 22 cases were biopsied specimen, in which only small volumes of viable tumor cells were available to interpret the IHC stained slide. Three-fourths of the endoscopically-biopsied gastric specimens also showed squeezing artifacts or tissue necrosis, which made it difficult to interpret the expressions of the IHC slides, particularly in weakly- and heterogeneously-stained cases. One case of non-GCB type determined by the Hans algorithm from a needle-biopsied specimen from the lymph node was re-assigned as a GCB type due to heterogeneity of the MUM1 expression. Our data suggest meaningful insights that IHC-based classification of COO

may lead to incorrect classification, particularly when assigning biopsied specimen containing small volumes of tumor cells or artifacts into GCB subtypes. However, this needs to be further evaluated in larger cohorts. Considering the study results suggesting that BCL6+ only Hans GCB cases show the highest discrepancy rate, careful evaluation is recommended in interpreting MUM1 expression, especially if the staining is weak and heterogenous in the biopsied specimen.

Unlike the binary IHC-based COO classification, there is a "type 3", or now known as the "unclassified" group in the GEP-based classification (11, 31, 32). This is a biologically distinct subgroup that does not express either sets of gene expression signatures (11, 31). Previous studies reported that this "unclassified" group comprises about 10-15% (32) and 22% (11) with intermediate prognoses between the GCB and ABC type (11, 17, 18). We evaluated some characteristics of the unclassified type, and extranodal lymphoma seem to exhibit statistically significant proportions (z-score = 2.13, p = 0.033) than nodal lymphoma. The proportion of the non-GCB type determined by the Hans algorithm was larger than the GCB type (n = 13 vs n = 10) without statistical significance. Moreover, 12 out of the 13 cases showed high levels of MUM1 expression in the non-GCB type (level of expression range, 30-95%).

The previous study conducted by Yoon *et al*. (14) analyzed the prognosis of the unclassified group as determined by the Lymph2Cx assay (n = 5, 6.1%), which revealed the worst outcome. However, another study by Barrans *et al*. (31) demonstrated the best survival in patients with the unclassified type of DLBCL. They speculated that this disagreement with previous GEP studies (11) may have probably arisen due to underlying diseases (14) or the inclusion of

a number of different entities in their cohort (31). Overall, this group was associated with low classifier gene expression, accompanied by an increase in T-cell associated genes (31). That is, this group includes cases where the B-cell signature is diluted by T-cells or non-hematological tissues. Therefore, a number of different entities are likely to be included in this unclassified group, such as DLBCL of T-cell rich type and DLBCL presenting in extranodal sites (31). The results of our study corroborate this and showed that the proportion of the extranodal site specimens was significantly higher than the nodal site specimens (z-score = 2.13, p = 0.033). These results may reflect the heterogeneity of the DLBCL population even though the unclassified group comprised small proportion.

The limitation of our study is that subgroups of cases are composed of relatively small proportions, that there is a possibility that they may not be representative. Therefore, further evaluation in larger cohorts is needed to determine the genetic mutation landscape of unclassified cases and to ascertain whether they represent a unique biologic group (32). Additionally, the retrospective design of the study resulted in a short follow-up period in evaluating the appropriate correlation with the survival rate.

In the era of precision medicine, accurate and reproducible assignment of COO in DLBCL patients has become important, not only for the ability to decide on targeted treatment, but also for its value as a prognostic indicator and in designing clinical trials of novel targeted agents. Since Scott *et al.* (17) developed the NanoString based platform called Lymph2Cx, several studies demonstrated its high concordance with the GEP-based assay and its better independent prognostic indicator abilities. In the hope of

using assays that provide more reliable and consistent COO assignment, we analyzed the discordant group cases between the Lymph2Cx assay and Hans algorithm, and the unclassified group cases determined by the Lymph2Cx assay. Our study analyzed overall discrepancy rate and discrepancy rate based on clinicopathologic and IHC profile features. Of note, IHC profile of CD10-/BCL6+/MUM1- and biopsied tissue specimen containing artifact or necrosis need careful assigning in COO into GCB type. Results of our study may provide useful guidelines in determining the COO in DLBCL patients.

V. Conclusion

Determining the COO of DLBCL is becoming more important with the introduction of novel therapies that selectively target the biological activities of GCB or ABC types of DLBCL. Lymph2Cx is a method that accurately determining COO by using 20 selected genes but there is discrepancy between determining COO by IHC method. We retrospectively analyzed 179 cases of DLBCL, in which the COOs were classified by the Lymph2Cx assay the Hans algorithm using combined IHC staining results for CD10, BCL6, and MUM1 antibodies on FFPE tissues. Diagnostic performance of the two methods were analyzed. Overall agreement was 134 (74.9%) and the proportion of discordant cases was higher in GCB type determined by the Hans algorithm (20.7% vs 8.3%). Of 22 discordant cases, none of the clinicopathologic characteristics comprised significantly higher proportion except for the COO classification by the Hans algorithm. Specifically, GCB type determined by the Hans algorithm comprised significant proportion than non-GCB type. Of 179 cases, Lymph2Cx categorized 23 cases (12.9%) as intermediate/unclassified type. The proportion of extranodal lymphoma was significantly higher than nodal lymphoma. The discrepancy rate in notable clinicopathologic characteristics was evaluated based on the clinicopathologic features of the discordant cases and Lymph2Cx unclassified cases. With regard to the discrepancy rate of the IHC profiles, CD10-/BCL6+/MUM1- (BCL6 only positive) GCB type by Hans algorithm revealed the highest discrepancy rate (66.7%) when compared to other IHC profiles. In the hope of using assays that provide more reliable and consistent COO assignment, we analyzed the discordant group cases between the Lymph2Cx assay and Hans algorithm, and the

unclassified group cases determined by the Lymph2Cx assay. Of note, IHC profile of CD10-/BCL6+/MUM1- and biopsied tissue specimen containing artifact or necrosis need careful assigning in COO into GCB type. Our study results may provide useful guidelines in determining the COO in DLBCL patients.

References

1. Frick M, Dorken B, Lenz G. The molecular biology of diffuse large B-cell lymphoma. Therapeutic advances in hematology. 2011;2(6):369-79.
2. Coiffier B. Diffuse large cell lymphoma. Current opinion in oncology. 2001;13(5):325-34.
3. Jaffe ES, Arber DA, Campo E, Harris NL, Quintanilla-Martinez L. Hematopathology, 2nd ed. Elsevier. 2017. Ch. 23.
4. Alizadeh AA, Eisen MB, Davis RE, Ma C, Lossos IS, Rosenwald A, *et al*. Distinct types of diffuse large B-cell lymphoma identified by gene expression profiling. Nature. 2000;403(6769):503-11.
5. Lenz G, Wright GW, Emre NC, Kohlhammer H, Dave SS, Davis RE, *et al*. Molecular subtypes of diffuse large B-cell lymphoma arise by distinct genetic pathways. Proceedings of the National Academy of Sciences of the United States of America. 2008;105(36):13520-5.
6. Lenz G, Wright G, Dave SS, Xiao W, Powell J, Zhao H, *et al*. Stromal gene signatures in large-B-cell lymphomas. N Engl J Med. 2008;359(22):2313-23.
7. Davis RE, Ngo VN, Lenz G, Tolar P, Young RM, Romesser PB, *et al*. Chronic active B-cell-receptor signalling in diffuse large B-cell lymphoma. Nature. 2010;463(7277):88-92.
8. Wilson WH, Young RM, Schmitz R, Yang Y, Pittaluga S, Wright G, *et al*. Targeting B cell receptor signaling with ibrutinib in diffuse large B cell lymphoma. Nature medicine. 2015;21(8):922-6.
9. Nowakowski GS, Chiappella A, Witzig TE, Spina M, Gascoyne RD, Zhang L, *et al*. ROBUST: Lenalidomide-R-CHOP versus placebo-R-CHOP in previously untreated ABC-type diffuse large B-cell lymphoma. Future oncology (London, England). 2016;12(13):1553-63.

10. Nowakowski GS, LaPlant B, Macon WR, Reeder CB, Foran JM, Nelson GD, *et al*. Lenalidomide combined with R-CHOP overcomes negative prognostic impact of non-germinal center B-cell phenotype in newly diagnosed diffuse large B-Cell lymphoma: a phase II study. Journal of clinical oncology : official journal of the American Society of Clinical Oncology. 2015;33(3):251-7.
11. Rosenwald A, Wright G, Chan WC, Connors JM, Campo E, Fisher RI, *et al*. The use of molecular profiling to predict survival after chemotherapy for diffuse large-B-cell lymphoma. N Engl J Med. 2002;346(25):1937-47.
12. Gutierrez-Garcia G, Cardesa-Salzmann T, Climent F, Gonzalez-Barca E, Mercadal S, Mate JL, et al. Gene-expression profiling and not immunophenotypic algorithms predicts prognosis in patients with diffuse large B-cell lymphoma treated with immunochemotherapy. Blood. 2011;117(18):4836-43.
13. Wright G, Tan B, Rosenwald A, Hurt EH, Wiestner A, Staudt LM. A gene expression-based method to diagnose clinically distinct subgroups of diffuse large B cell lymphoma. Proceedings of the National Academy of Sciences of the United States of America. 2003;100(17):9991-6.
14. Yoon N, Ahn S, Yong Yoo H, Jin Kim S, Seog Kim W, Hyeh Ko Y. Cell-of-origin of diffuse large B-cell lymphomas determined by the Lymph2Cx assay: better prognostic indicator than Hans algorithm. Oncotarget. 2017;8(13):22014-22.
15. Hans CP, Weisenburger DD, Greiner TC, Gascoyne RD, Delabie J, Ott G, et al. Confirmation of the molecular classification of diffuse large B-cell lymphoma by immunohistochemistry using a tissue microarray. Blood. 2004;103(1):275-82.
16. Choi WW, Weisenburger DD, Greiner TC, Piris MA, Banham AH, Delabie J, et al. A new immunostain algorithm classifies diffuse

large B-cell lymphoma into molecular subtypes with high accuracy. Clinical cancer research : an official journal of the American Association for Cancer Research. 2009;15(17):5494-502.

17. Scott DW, Wright GW, Williams PM, Lih C-J, Walsh W, Jaffe ES, et al. Determining cell-of-origin subtypes of diffuse large B-cell lymphoma using gene expression in formalin-fixed paraffin-embedded tissue. Blood. 2014;123(8):1214-7.

18. Scott DW, Mottok A, Ennishi D, Wright GW, Farinha P, Ben-Neriah S, et al. Prognostic Significance of Diffuse Large B-Cell Lymphoma Cell of Origin Determined by Digital Gene Expression in Formalin-Fixed Paraffin-Embedded Tissue Biopsies. Journal of clinical oncology : official journal of the American Society of Clinical Oncology. 2015;33(26):2848-56.

19. Phang KC, Akhter A, Tizen NMS, Rahman FA, Zahratul Azma R, Elyamany G, et al. Comparison of protein-based cell-of-origin classification to the Lymph2Cx RNA assay in a cohort of diffuse large B-cell lymphomas in Malaysia. Journal of clinical pathology. 2017.

20. Swerdlow SH, Campo E, Pileri SA, Harris NL, Stein H, Siebert R, et al. The 2016 revision of the World Health Organization classification of lymphoid neoplasms. Blood. 2016;127(20):2375-90.

21. Barton S, Hawkes EA, Wotherspoon A, Cunningham D. Are we ready to stratify treatment for diffuse large B-cell lymphoma using molecular hallmarks? The oncologist. 2012;17(12):1562-73.

22. Veldman-Jones MH, Brant R, Rooney C, Geh C, Emery H, Harbron CG, et al. Evaluating Robustness and Sensitivity of the NanoString Technologies nCounter Platform to Enable Multiplexed Gene Expression Analysis of Clinical Samples. Cancer research. 2015;75(13):2587-93.

23. Reis PP, Waldron L, Goswami RS, Xu W, Xuan Y, Perez-Ordonez B,

et al. mRNA transcript quantification in archival samples using multiplexed, color-coded probes. BMC biotechnology. 2011;11:46.

24. Scott DW, Chan FC, Hong F, Rogic S, Tan KL, Meissner B, et al. Gene expression-based model using formalin-fixed paraffin-embedded biopsies predicts overall survival in advanced-stage classical Hodgkin lymphoma. Journal of clinical oncology : official journal of the American Society of Clinical Oncology. 2013;31(6):692-700.

25. Geiss GK, Bumgarner RE, Birditt B, Dahl T, Dowidar N, Dunaway DL, et al. Direct multiplexed measurement of gene expression with color-coded probe pairs. Nature biotechnology. 2008;26(3):317-25.

26. Jais JP, Molina TJ, Ruminy P, Gentien D, Reyes C, Scott DW, et al. Reliable subtype classification of diffuse large B-Cell lymphoma samples from GELA LNH2003 trials using the Lymph2Cx gene expression assay. Haematologica. 2017.

27. Meyer PN, Fu K, Greiner TC, Smith LM, Delabie J, Gascoyne RD, et al. Immunohistochemical methods for predicting cell of origin and survival in patients with diffuse large B-cell lymphoma treated with rituximab. Journal of clinical oncology : official journal of the American Society of Clinical Oncology. 2011;29(2):200-7.

28. de Jong D, Rosenwald A, Chhanabhai M, Gaulard P, Klapper W, Lee A, et al. Immunohistochemical prognostic markers in diffuse large B-cell lymphoma: validation of tissue microarray as a prerequisite for broad clinical applications--a study from the Lunenburg Lymphoma Biomarker Consortium. J Clin Oncol. 2007;25(7):805-12.

29. Fu K, Weisenburger DD, Choi WW, Perry KD, Smith LM, Shi X, et al. Addition of rituximab to standard chemotherapy improves the survival of both the germinal center B-cell-like and non-germinal center B-cell-like subtypes of diffuse large B-cell lymphoma. Journal of clinical oncology : official journal of the American

Society of Clinical Oncology. 2008;26(28):4587-94.

30. Ott MM, Horn H, Kaufmann M, Ott G. The Hans classificator does not predict outcome in diffuse large B cell lymphoma in a large multicenter retrospective analysis of R-CHOP treated patients. Leukemia research. 2012;36(5):544-5.

31. Barrans SL, Crouch S, Care MA, Worrillow L, Smith A, Patmore R, et al. Whole genome expression profiling based on paraffin embedded tissue can be used to classify diffuse large B-cell lymphoma and predict clinical outcome. British journal of haematology. 2012;159(4):441-53.

32. Scott DW. Cell-of-Origin in Diffuse Large B-Cell Lymphoma: Are the Assays Ready for the Clinic? American Society of Clinical Oncology educational book American Society of Clinical Oncology Meeting. 2015:e458-66

Supplementary Table. Mentionable cases in the discordant group

Case	Age/Sex	Bx site	Bx type	CD10 (%)	BCL6 (%)	MUM1 (%)	Hans Algorithm	Lymph2Cx	Comment
1	70/M	Stomach	Endoscopic	- (0)	+ (50)	+ (30)	non-GCB	GCB	Tissue insufficient for interpretation Heterogenous MUM1 expression
2	60/F	Stomach	Endoscopic	- (0)	+ (90)	+ (30)	non-GCB	GCB	Tissue necrosis
3	33/F	Stomach	Endoscopic	- (0)	+ (90)	+ (30)	non-GCB	GCB	Tissue with squeezing artifact Weak & heterogenous MUM1 expression
4	81/M	Chest wall	Excisional	- (0)	+ (30)	+ (30)	non-GCB	GCB	Tissue necrosis
5	41/M	Lymph Node	Needle	- (0)	+ (60)	+ (30)	non-GCB	GCB	MUM1 misinterpretation (30%->15%) due to weak & heterogenous MUM1 expression
6	66/M	Lymph Node	Endoscopic	- (0)	+ (80)	- (20)	GCB	ABC	
7	61/M	Nasal cavity	Endoscopic	+ (>30)	- (<30)	- (10)	GCB	ABC	
8	74/M	Lymph Node	Needle	- (0)	+ (80)	- (20)	GCB	ABC	

Note: COO, cell of origin; ABC, activated B cell; GCB, germinal center B cell; Bx, biopsy